Ghost Channels and Ghost Cycles Guiding Long Transients in Dynamical Systems

D. Koch,[1,*] A. Nandan,[1,*] G. Ramesan,[1] I. Tyukin,[2,3] A. Gorban,[4] and A. Koseska[1,†]
[1]Cellular computations and learning, Max Planck Institute for Neurobiology of Behavior—caesar, Bonn, Germany
[2]Department of Mathematics, King's College, London, United Kingdom
[3]Skolkovo Institue of Science and Technology, Moscow, 121205, Russia
[4]Department of Mathematics, University of Leicester, Leicester, United Kingdom

(Received 11 October 2023; revised 30 April 2024; accepted 4 June 2024; published 25 July 2024)

Dynamical descriptions and modeling of natural systems have generally focused on fixed points, with saddles and saddle-based phase-space objects such as heteroclinic channels or cycles being central concepts behind the emergence of quasistable long transients. Reliable and robust transient dynamics observed for real, inherently noisy systems is, however, not met by saddle-based dynamics, as demonstrated here. Generalizing the notion of ghost states, we provide a complementary framework that does not rely on the precise knowledge or existence of (un)stable fixed points, but rather on slow directed flows organized by ghost sets in *ghost channels* and *ghost cycles*. Moreover, we show that the appearance of these novel objects is an emergent property of a broad class of models typically used for description of natural systems.

DOI: 10.1103/PhysRevLett.133.047202

Living and man-made, but also ecological or climate systems are classically described to reproduce asymptotic behavior, implying that the observed dynamics is retained indefinitely in absence of a perturbation. Mathematically, such dynamics corresponds to invariant sets that represent objects in phase space, the simplest being stable fixed points separated by separatrixes of saddles [1,2]. However, a growing body of empirical evidence suggests that real-world systems are often characterized by long transients which are not invariant, are quasistable, and the system switches between them. The duration of the quasistable patterns is much longer than one would expect from the characteristic elementary processes, whereas the switching is triggered by external signals or system autonomously, and occurs on a timescale much shorter than the one of the preceding dynamical pattern. Examples include dynamics of neuronal activity [3–5], camouflaging in animals [6], cell signaling [7–9], ecological [10,11], earth and climate systems [12,13], replicator networks [14], semiconductor lasers, and Josephson junctions [15]. In the context of neuronal systems, the described dynamics is often referred to as *metastable* [16–19]. From the aspect of topological dynamics, long transients are caused by the bifurcations (explosions) of ω-limit sets or through the occurrence of generalized homoclinic (loop) structures [20–22]. In particular, the emergence of long transients has been conceptualized by trapping the system's dynamics in the vicinity of a saddle [10] [Fig. 1(a)], or a saddle-node "ghost" [7,8,10,22] [Fig. 1(b)], whereas the switching is thought to occur via saddle-based heteroclinic structures [23–27] [Fig. 1(c)].

In this Letter, we complement the topological theory with novel structures. Generalizing the concept of ghost states [2,15,22], we provide a theoretical framework for generation of sequential quasistable dynamics that does not rely on (un)stable fixed points, but on slow directed phase-space flows guided by *ghost channels* and *ghost cycles*

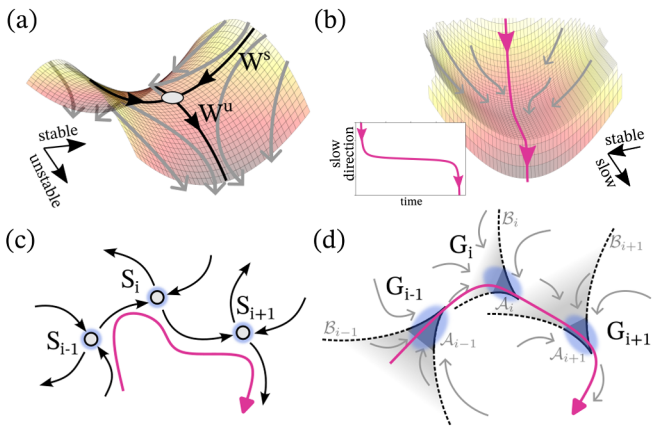

FIG. 1. Schematics of phase-space objects. (a) Quasipotential landscape of a saddle fixed point. Gray dot: unstable fixed point localization. (b) Quasipotential landscape of a ghost state. Note the absence of a fixed point. Inset: time course of a trajectory with slow transition through the ghost. Schematic diagrams of scaffolds of connected (c) saddles (S_i), i.e., heteroclinic channel, and (d) ghosts (G_i), i.e., ghost channel. A_i denotes the ghost-attracting set of G_i, and B_i its basin. (a)–(d) Black, gray, and magenta arrows represent (un)stable manifolds, flow direction and example trajectories, respectively.

*These authors contributed equally to this letter.
†Contact author: aneta.koseska@mpinb.mpg.de

[Fig. 1(d)]. We identify the criteria for their emergence, and demonstrate that ghost-based scaffolds capture properties of long transients in noisy systems better than traditional models relying on invariant sets.

Properties of ghost sets—To formally define ghost channels and cycles, we need to provide a quantitative description of ghost sets, their boundaries, and trapping times. Consider a conceptual 2D system of first order differential equations $\dot{\mathbf{x}} = \mathbf{F}(\mathbf{x})$ given by

$$\dot{x} = \alpha + x^2, \quad \dot{y} = -y. \tag{1}$$

For $\alpha < 0$, a stable fixed point and a dissipative saddle coexist, whereas for $\alpha \to 0^+$, a ghost state or a "bottleneck" appears [2] [Supplemental Material [28] Fig. S1(a), numerical analysis as in Ref. [29]].

Fixed points in dynamical systems (and their surrounding regions of slow dynamics) can be identified using an auxiliary scalar function $q(\mathbf{x}) = \frac{1}{2}|\mathbf{F}(\mathbf{x})|^2$, which is also a Lyapunov function, related to the system's kinetic energy [30] where $|.|$ is the standard Euclidean norm. Calculating the kinetic energy for system Eqs. (1) shows that $q(\mathbf{x}^*) = 0$ if and only if x^* is a fixed point, i.e., the saddle [Fig. 2(a), top; the stable fixed point is omitted for brevity]. In its proximity q adopts values close to 0 ($q_{\text{thresh}} = 10^{-2}$), corresponding to the upper surface of the saddle [Fig. 1(a)]. Slow dynamics with $q < q_{\text{thresh}}$ still occurs for $\alpha \to 0^+$, spanning across an even larger phase-space area [Fig. 2(b), top]. This area corresponds to the shallow-slope region of the ghost state in Fig. 1(b). If the norm of the dynamics is close to zero ($q_{\text{thresh}} = 10^{-2}$), local linear expansion is still valid [30]. Numerically evaluating the two local eigenvalues, $\lambda^{sp}_{\max}$ and $\lambda^{sp}_{\min}$, for every slow point (x^{sp}, y^{sp}) satisfying $q(x^{sp}, y^{sp}) < q_{\text{thresh}}$ using the Jacobian of Eqs. (1) shows that $\lambda^{sp}_{\min}$ is negative for $\alpha < 0$ and $\alpha \to 0^+$ in the whole slow region [Supplemental Material [28], Sec. I, Fig. S1(b)]. $\lambda^{sp}_{\max}$, however, remains positive around the saddle as characteristic for unstable fixed points, while for $\alpha \to 0^+$ the $\lambda^{sp}_{\max}$ changes from negative to positive in the slow-dynamics region [Figs. 2(a) and 2(b), bottom]. The corresponding eigenvectors thereby determine the flow direction: trajectories starting along the stable saddle manifold are deflected along its unstable manifold, whereas for $\alpha \to 0^+$ the phase space flow attracts and guides the trajectories along the low kinetic energy area [Figs. 2(a) and 2(b), bottom, respectively]. Thus, the system's trajectories, although transiently attracted to the ghost state, eventually escape. This is also contrary to a saddle node (i.e., when saddle and stable fixed point collide at $\alpha = 0$), as the trajectories coming from the left will be trapped at the origin.

Since the trajectories in the ghost travel along phase space region where $\lambda^{sp}_{\max} \approx 0$, we investigated how the trapping times, and thereby the effective quasistability of the ghost differs to that of the saddle. For this, we divided each trajectory into N segments, explicitly integrated system Eqs. (1) along each segment [between initial and final $(x_{\text{in,i}}, y_{\text{in,i}})/(x_{\text{fin,i}}, y_{\text{fin,i}})$ points; Supplemental Material [28], Sec. II], and determined analytically and numerically the local trapping times τ_i as a function of the local $\lambda^{sp}_{\max}$. The functional forms of the analytical expressions,

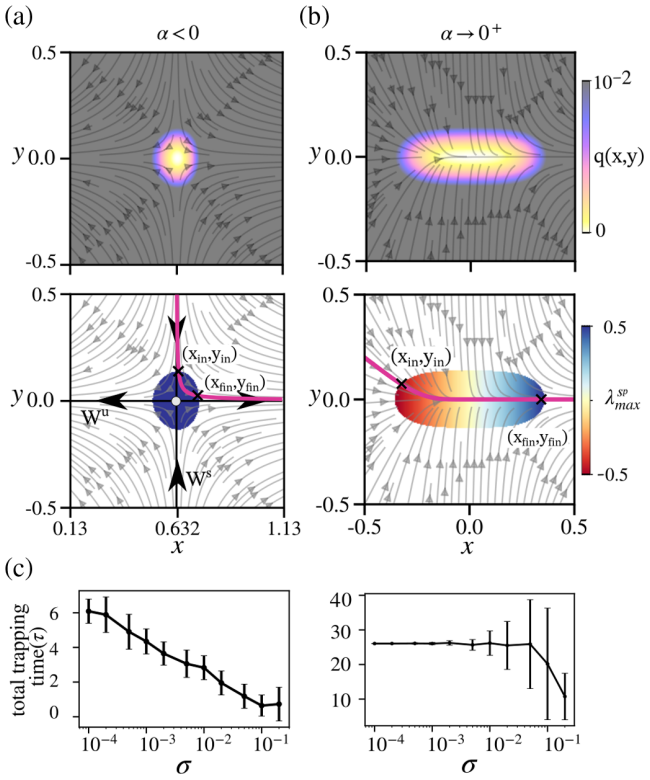

FIG. 2. Characteristics of quasistable transients emerging from saddles vs ghost states. (a) Top: Kinetic energy estimate $[q(x, y)]$ around a saddle fixed point $[\alpha = -0.4$ in Eq. (1)]; Bottom: corresponding maximum eigenvalue $(\lambda^{sp}_{\max})$ in the $q(x^{sp}, y^{sp}) < q_{\text{thresh}} = 0.01$ region; Stable/unstable (W^s, W^u) manifold (black arrow lines) and exemplary phase space trajectory (magenta line). Black crosses: entry and exit points; (b) Same as in (a), but for ghost state $[\alpha = 0.01$ in Eqs. (1)]. Gray arrow lines: phase space flow. (c) Dependence of the total trapping time in the $q(x^{sp}, y^{sp}) < q_{\text{thresh}}$ region of the saddle (left) and the ghost (right) for different additive noise intensities σ. Mean ± s.d. from 30 repetitions are shown. See Supplemental Material [28].

$$\tau_{i,\text{saddle}} = \frac{1}{\lambda^{sp}_{\max}} \left[\ln \left| \frac{x - \lambda^{sp}_{\max}/2}{x + \lambda^{sp}_{\max}/2} \right| \right] \Bigg|_{x_{\text{in,i}}}^{x_{\text{fin,i}}}$$

and

$$\tau_{i,\text{ghost}} = \frac{2}{\lambda^{sp}_{\max}} \left[\tan^{-1} \left(\frac{2x}{\lambda^{sp}_{\max}} \right) \right] \Bigg|_{x_{\text{in,i}}}^{x_{\text{fin,i}}}$$

and the corresponding numerical verification show that τ_i quickly decays along positive $\lambda^{sp}_{\max}$ for the saddle, whereas for the ghost, a parabolic dependency on $\lambda^{sp}_{\max}$ applies [Supplemental Material [28] Fig. S1(d)]. Contrary to the saddle, for which τ decreases monotonically with

increasing σ, for the ghost, τ is robust with respect to noise [31], remaining constant over 2 orders of magnitude of σ and decaying to half-maximum only at $\sigma \sim 10^{-1}$. This characteristic of ghost sets is preserved for different α values [Supplemental Material [28] Fig. S1(e)].

Following the features from this example, we now define *ghost attracting sets* formally. $\mathcal{A}$ is a ghost attracting set if (a) it is a closed bounded set that does not contain any semitrajectories in forward time; (b) there is a closed set $\mathcal{B}(\mathcal{A})$ with nonempty interior, the ghost basin of attraction, associated with $\mathcal{A}$, such that (i) for any $x_0 \in \mathcal{B}(\mathcal{A})$ there is a $t(x_0) \geq 0$ such that $x(t; x_0) \in \mathcal{A}$ (attraction); (ii) for any $x_0 \in \mathcal{A}$ there is a $t(x_0) \leq 0$ such that $x(t; x_0) \in \mathcal{B}(\mathcal{A})$ (minimality); (iii) $\mathcal{A}$ is a proper subset of $\mathcal{B}(\mathcal{A})$ (contraction). Moreover, $\mathcal{A}$ has entrance and exit boundaries with respect to the flow [32].

Ghost channels and ghost cycles—We next extend the concept of ghost sets to complex ghost structures that we term *ghost channels* and *ghost cycles*, in analogy to heteroclinic structures constructed from saddles. Formally, we define a ghost channel as follows:

Let $\mathcal{A}_1, \ldots, \mathcal{A}_N$ be N ghost attracting sets of the underlying system. We say that the sets form a ghost channel if

$$\partial_{\text{esc}}\mathcal{A}_i \subset \mathcal{B}(\mathcal{A}_{i+1}), \quad i = 1, \ldots, N-1, \tag{2}$$

where $\partial_{\text{esc}}\mathcal{A}_i$ is the escape boundary of $\mathcal{A}_i$ with respect to the flow. Thus, ghost channels (GChs) appear when multiple ghosts are aligned in a sequence such that the trajectory escaping a preceding ghost is directed by the flow through the next ghost in the sequence [Figs. 1(d) and 3(b); Supplemental Material [28], Sec. III. B and Ref. [32]]. Thus, GChs, in accordance to their definition, inherit attraction, whereas heteroclinic channels (HCh) may not. Comparing the reproducible guidance of trajectories through a GCh and a HCh [Fig. 3(a)], both constructed geometrically [33,34] for simplicity, shows that only the GCh uniquely funnels the flow in phase space, even for increased σ [Fig. 3(b); Supplemental Material [28] Figs. S2(a)–S2(d)]. In contrast, the trajectories stochastically exit along the HCh's unstable manifold. This shows that GChs, but not HChs, guarantee reproducible quasistable sequential switching dynamics, as also confirmed by the consistently lower Euclidean distance between the trajectories in the GCh [Fig. 3(c)]. We find that GChs with equivalent properties are characteristic for a broad class of systems, including models of charge density waves [15], climate tipping cascades [35], and unidirectionally coupled cellular signaling model [36] [Supplemental Material [28] Fig. S2(e), Sec. III. B].

To conceptualize the emergence of oscillatory quasistable sequential dynamics, we also constructed ghost cycles [GC; Fig. 4(e)]. Formally, if $\partial_{\text{esc}}\mathcal{A}_N \subset \mathcal{B}(\mathcal{A}_1)$, we have a GC. To compare their dynamics to heteroclinic cycles [HC; Fig. 4(a)], we matched the trapping times

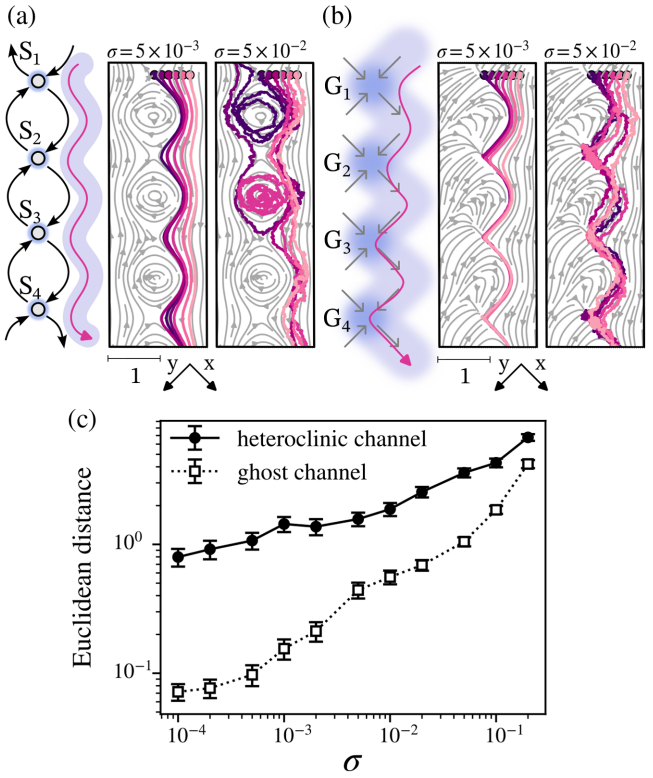

FIG. 3. Comparison of heteroclinic (HCh) and ghost (GCh) channels' dynamics. (a) Schematic of a HCh and exemplary trajectories for six initial conditions and two different noise intensities σ. (b) Same as in (a), but for a GCh. (c) Euclidean distance between pairwise trajectories in the HCh or GCh as a function of σ (mean $\pm$SEM from 180 trajectories: six initial conditions with 30 repetitions; Supplemental Material [28]).

(in arbitrary units) along a single saddle and ghost to be similar at low σ by adjusting the saddle values of a generic noise-driven Lotka-Volterra HC model (Supplemental Material [28] Fig. S3). The period of the HC [37], $T \sim |\ln\sigma|/\lambda_u$ decreases almost exponentially as σ is increased, following the decrease of the total trapping time at the saddles [Figs. 4(b) and 4(d)]. Moreover, the intervals in which the system's dynamics spends switching between the saddles within one HC period dominates already for intermediate noise $\sigma \leq 10^{-3}$. This is also reflected in the speed of the phase-space trajectories, which increasingly fill in the phase-space regions distant to the heteroclinic backbone under increased noise [Fig. 4(c)]. In contrast, increasing σ does not affect the mean period of GCs over a large range of noise intensity, and the trajectories remain bounded along the cycle [Figs. 4(f)–4(h)]. The times spent on the ghosts remain $\sim$ twofold larger than the transition times between them, even for $\sigma > 10^{-2}$. This is also reflected in the speed of the trajectory in phase space, with a clear separation of the timescales [Fig. 4(g)]. GCs thus uniquely provide a dynamical basis for emergence of robust and sustained quasistable oscillatory switching dynamics even for

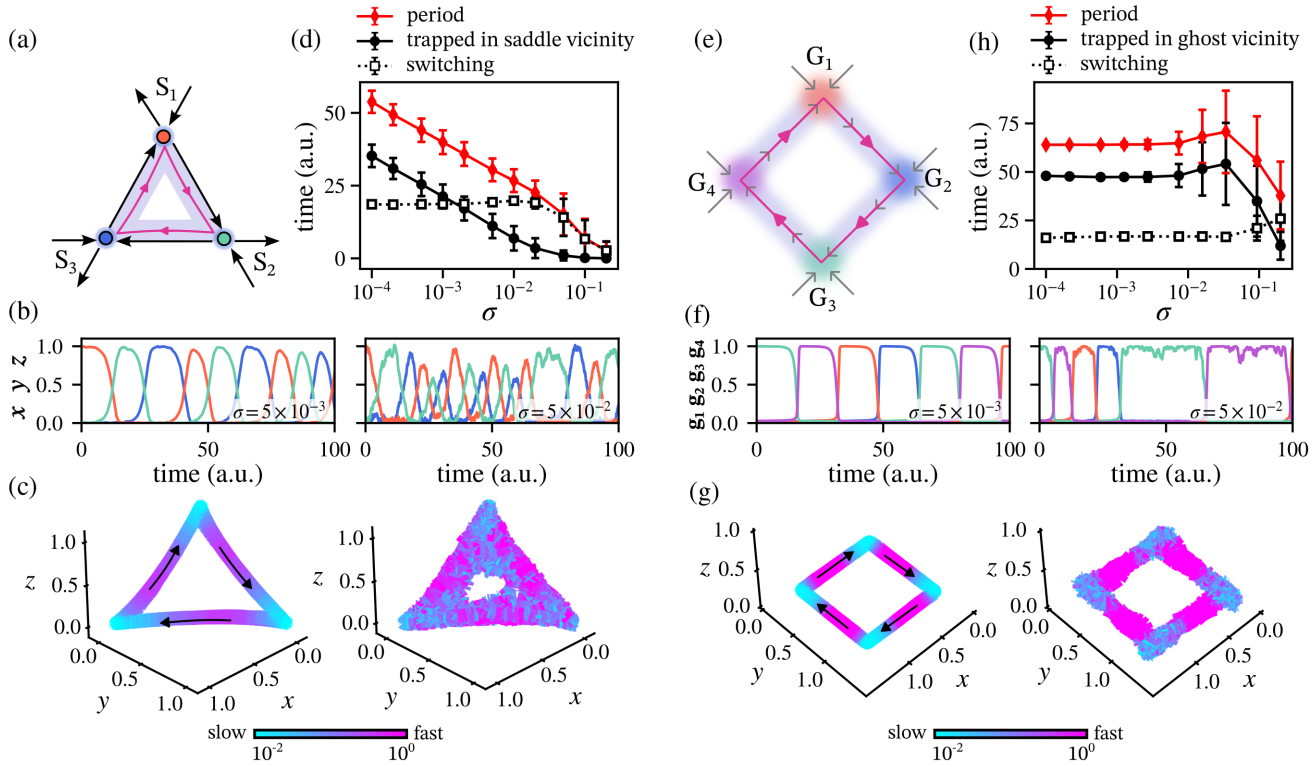

FIG. 4. Comparison of heteroclinic (HC) and ghost (GC) cycles. (a) Schematic of a HC of three saddles (S_1 to S_3) and (b) exemplary time series for two noise intensities σ. (c) Corresponding phase-space trajectories, color coded by velocity. (d) Characteristic HC times as a function of σ: HC period (red), total trapping time at the saddles (solid black) and switching time (dashed black line). Vicinity was determined by three-dimensional spheres of radius $\epsilon = 0.1$ centered around the saddles. The mean $\pm$ root mean squared error of the s.d. over time is plotted from 30 trajectories. (e)–(g) Same as in (a)–(c), but for a GC (ghosts G_1 to G_4). (h) Characteristic GC times as a function of σ. Labeling as in (d).

inherently noisy systems. In models, GCs can occur when a limit cycle terminates via a single or multiple saddle node on invariant circle bifurcations (SNICs) [38–40]. In the vicinity of the SNICs, the system's dynamics is governed by the SNs about to emerge: after being transiently trapped in the ghost set, the trajectory escapes and is trapped by the next one, thus continually switching between ghosts in the sequence [Supplemental Material [28], Figs. S5(a)–S5(c)]. We demonstrate this also for a generic gene-regulatory network model proposed to underlie stem cell differentiation [39] [Supplemental Material [28], Figs. S5(d)–S5(f)].

Conclusions and outlook—We introduced ghost channels and ghost cycles as novel objects that guide flow in phase space and give rise to reliable quasistable dynamics even in the presence of noise. This shows that quasistability can emerge in systems whose dynamics is neither organized by fixed points, nor dominated by limit cycle attractors (slow-fast systems [1,41,42]), the comparison to which we discussed elsewhere [43]. We thus propose that ghost-based objects provide a possible mechanistic description for the emergence of ordered and reproducible transient behavior across living and manmade systems [3,4,6,10,12,44,45]. Using mainly geometric models to derive the basic definitions here, we identified the dynamical characteristics ($q \sim 0$, eigenvalue gradient and escape paths), which could be used in an algorithmic fashion to identify ghost sets in any arbitrary-dimensional complex system.

The proposed concepts could potentially provide a way forward in identifying mechanisms, e.g., of emergence of complex low-dimensional manifolds [46] typical for neuronal activity data during cognitive or behavioral tasks [33,44,45], as it is easy to imagine hybrid structures of ghosts and saddles giving rise to new phase-space objects benefiting from different properties (Supplemental Material [28], Fig. S6). Moreover, the presence of distinct timescales emerging from the ghost scaffolds could aid development of time-series analysis methods for detecting quasistable patterns and corresponding transitions, e.g., via phase-space-based metrics [47]. Our conceptual framework therefore provides new perspectives on natural systems where long transients are common.

Acknowledgments—We thank A. Aulehla, K. Lehnertz, and P. Francois for valuable feedback on the manuscript, and J. Gunawardena and J. Garcia-Ojalvo for insightful discussions. A. K. acknowledges funding by the Lise Meitner Excellence Programme of the Max Planck Society, D. K—EMBO Fellowship (Grant No. ALTF 310-2021), I. T—UKRI Turing AI Fellowship EP/V025295/2.

[1] J. Guckenheimer and P. Holmes, *Nonlinear Oscillations, Dynamical Systems, and Bifurcations of Vector Fields* (Springer, New York, 1983).

[2] S. H. Strogatz, *Nonlinear Dynamics and Chaos: With Applications to Physics, Biology, Chemistry and Engineering* (Westview Press, Cambridge, 2000).

[3] O. Mazor and G. Laurent, Transient dynamics versus fixed points in odor representations by locust antennal lobe projection neurons, Neuron **48**, 661 (2005).

[4] D. Benozzo, G. L. Camera, and A. Genovesio, Slower prefrontal metastable dynamics during deliberation predicts error trials in a distance discrimination task, Cell Rep. **35**, 108934 (2021).

[5] S. Recanatesi, U. Pereira-Obilinovic, M. Murakami, Z. Mainen, and L. Mazzucato, Metastable attractors explain the variable timing of stable behavioral action sequences, Neuron **110**, 139 (2022).

[6] T. Woo, X. Liang, D. A. Evans, O. Fernandez, F. Kretschmer, S. Reiter, and G. Laurent, The dynamics of pattern matching in camouflaging cuttlefish, Nature (London) **619**, 122 (2023).

[7] A. Nandan, A. Das, R. Lott, and A. Koseska, Cells use molecular working memory to navigate in changing chemoattractant fields, eLife **11**, e76825 (2022).

[8] O. Karin, E. A. Miska, and B. D. Simons, Epigenetic inheritance of gene silencing is maintained by a self-tuning mechanism based on resource competition, Cell Syst. **14**, 24 (2023).

[9] D. E. Tufcea and P. François, Critical timing without a timer for embryonic development, Biophys. J. **109**, 1724 (2015).

[10] A. Hastings, K. C. Abbott, K. Cuddington, T. Francis, G. Gellner, Y.-C. Lai, A. Morozov, S. Petrovskii, K. Scranton, and M. L. Zeeman, Transient phenomena in ecology, Science **361**, eaat6412 (2018).

[11] C. Bieg, H. Vallès, A. Tewfik, B. E. Lapointe, and K. S. McCann, Toward a multi-stressor theory for coral reefs in a changing world, Ecosystems **27**, 310 (2024).

[12] A. C. de Verdière, A simple model of millennial oscillations of the thermohaline circulation, J. Phys. Oceanogr. **37**, 1142 (2007).

[13] B. Kaszás, T. Haszpra, and M. Herein, The snowball earth transition in a climate model with drifting parameters: Splitting of the snapshot attractor, Chaos **29**, 113102 (2019).

[14] J. Sardanyés and R. V. Solé, Delayed transitions in nonlinear replicator networks: About ghosts and hypercycles, Chaos Solitons Fractals **31**, 305 (2007).

[15] S. H. Strogatz and R. M. Westervelt, Predicted power laws for delayed switching of charge-density waves, Phys. Rev. B **40**, 10501 (1989).

[16] J. A. S. Kelso, Multistability and metastability: Understanding dynamic coordination in the brain, Phil. Trans. R. Soc. B **367**, 906 (2012).

[17] G. Deco and M. Kringelbach, Metastability and coherence: Extending the communication through coherence hypothesis using a whole-brain computational perspective, Trends Neurosci. **39**, 432 (2016).

[18] K. L. Rossi, R. C. Budzinski, E. S. Medeiros, B. R. R. Boaretto, L. Muller, and U. Feudel, A unified framework of metastability in neuroscience, arXiv:2305.05328.

[19] A. Bovier and F. den Hollander, *Metastability: A Potential Theoretic Approach* (Springer International Publishing, New York, 2015).

[20] V. I. Elokhin, G. S. Yablonskii, A. N. Gorban, and V. M. Cheresiz, Dynamics of chemical reactions and nonphysical steady states, React. Kinet. Catal. Lett. **15**, 245 (1980).

[21] A. N. Gorban and V. M. Cheresiz, Slow relaxations of dynamical systems and bifurcations of ω-limit sets, J. Appl. Ind. Math. **4**, 55 (2010).

[22] A. N. Gorban, Singularities of transition processes in dynamical systems: Qualitative theory of critical delays, Electron. J. Diff. Equations Monograph **1**, 05 (2004).

[23] R. M. May and W. J. Leonard, Nonlinear aspects of competition between three species, SIAM J. Appl. Math. **29**, 243 (1975).

[24] M. Rabinovich, A. Volkovskii, P. Lecanda, R. Huerta, H. D. I. Abarbanel, and G. Laurent, Dynamical encoding by networks of competing neuron groups: Winnerless competition, Phys. Rev. Lett. **87**, 068102 (2001).

[25] C. Kirst and M. Timme, From networks of unstable attractors to heteroclinic switching, Phys. Rev. E **78**, 065201 (2008).

[26] A. D. Horchler, K. A. Daltorio, H. J. Chiel, and R. D. Quinn, Designing responsive pattern generators: Stable heteroclinic channel cycles for modeling and control, Bioinspiration Biomimetics **10**, 026001 (2015).

[27] P. Ashwin and C. Postlethwaite, On designing heteroclinic networks from graphs, Physica D (Amsterdam) **265**, 26 (2013).

[28] See Supplemental Material at http://link.aps.org/supplemental/10.1103/PhysRevLett.133.047202 for details of analytical derivations, model details and Supplemental Figures.

[29] B. Ermentrout, *Simulating, Analyzing, and Animating Dynamical Systems* (Society for Industrial and Applied Mathematics, 2002), 10.1137/1.9780898718195.

[30] D. Sussillo and O. Barak, Opening the black box: Low-dimensional dynamics in high-dimensional recurrent neural networks, Neural Comput. **25**, 626 (2013).

[31] J. Sardanyés, C. Raich, and T. Alarcón, Noise-induced stabilization of saddle-node ghosts, New J. Phys. **22**, 093064 (2020).

[32] I. Y. Tyukin, A. N. Gorban, R. Alsolamy, T. Tyukina, D. Koch, A. Koseska, and H. Nijmeijer, A simple extension of the method of Lyapunov and the notions of ghost attractors and ghost channels (to be published).

[33] M. Morrison and L.-S. Young, Chaotic heteroclinic networks as models of switching behavior in biological systems, Chaos **32**, 123102 (2022).

[34] F. Corson and E. D. Siggia, Geometry, epistasis, and developmental patterning, Proc. Natl. Acad. Sci. U.S.A. **109**, 5568 (2012).

[35] M. M. Dekker, A. S. von der Heydt, and H. A. Dijkstra, Cascading transitions in the climate system, Earth Syst. Dyn. **9**, 1243 (2018).

[36] J. E. Ferrell and S. H. Ha, Ultrasensitivity part III: Cascades, bistable switches, and oscillators, Trends Biochem. Sci. **39**, 612 (2014).

[37] M. I. Rabinovich, R. Huerta, and P. Varona, Heteroclinic synchronization: Ultrasubharmonic locking, Phys. Rev. Lett. **96**, 014101 (2006).

[38] M. W. Meeuse, Y. P. Hauser, L. J. M. Moya, G.-J. Hendriks, J. Eglinger, G. Bogaarts, C. Tsiairis, and H. Großhans, Developmental function and state transitions of a gene expression oscillator in Caenorhabditis elegans, Mol. Syst. Biol. **16**, e9498 (2020).

[39] S. Farjami, K. C. Sosa, J. H. P. Dawes, R. N. Kelsh, and A. Rocco, Novel generic models for differentiating stem cells reveal oscillatory mechanisms, J. R. Soc. Interface **18**, 20210442 (2021).

[40] P. G. L. Sanchez, V. Mochulska, C. M. Denis, G. Mönke, T. Tomita, N. Tsuchida-Straeten, Y. Petersen, K. Sonnen, P. François, and A. Aulehla, Arnold tongue entrainment reveals dynamical principles of the embryonic segmentation clock, eLife **11**, e79575 (2022).

[41] N. Fenichel, Persistence and smoothness of invariant manifolds for flows, Indiana University mathematics Journal **21**, 193 (1971).

[42] C. Kuehn, *Multiple Time Scale Dynamics* (Springer International Publishing, New York, 2015).

[43] D. Koch and A. Koseska, Ghost cycles exhibit increased entrainment and richer dynamics in response to external forcing compared to slow-fast systems, arXiv: 2403.19624.

[44] S. Kato, H. S. Kaplan, T. Schrödel, S. Skora, T. H. Lindsay, E. Yemini, S. Lockery, and M. Zimmer, Global brain dynamics embed the motor command sequence of caenorhabditis elegans, Cell **163**, 656 (2015).

[45] A. L. A. Nichols, T. Eichler, R. Latham, and M. Zimmer, A global brain state underlies C. elegans sleep behavior, Science **356**, eaam6851 (2017).

[46] C. Langdon, M. Genkin, and T. A. Engel, A unifying perspective on neural manifolds and circuits for cognition, Nat. Rev. Neurosci. **24**, 363 (2023).

[47] P. Graben and A. Hutt, Detecting recurrence domains of dynamical systems by symbolic dynamics, Phys. Rev. Lett. **110**, 154101 (2013).